

# Statistical theory of mixed-valence selectivity in biological ion channels

W.A.T. Gibby\*, M.L. Barabash\*, C. Guardiani\*, D.G. Luchinsky\*<sup>†</sup> and P.V.E. McClintock\*

\*Department of Physics,

Lancaster University, Lancaster, UK, LA1 4YB

Email: w.gibby@lancaster.ac.uk

<sup>†</sup>SGT Inc., Ames Research Center, Moffet field, CA, 94035, USA

Email: d.luchinsky@lancaster.ac.uk

**Abstract**—In this article we apply our multi-component statistical and linear response theory to the process of mixed-valence ionic transport in a biological sodium ion channel. We analyse the free energy spectra, and statistical fluctuations (which are proportional to the conductivity) to investigate conditions and optimal parameters required for selectivity.

## I. INTRODUCTION

Understanding, predicting, and controlling how ions permeate nanoscale pores is increasingly important in the fields of nano- and biophysics. Ionic transport governs a large and growing number of applications including, but not limited to, DNA sensing [1], water treatment [2] and natural gas purification [3]. In general the pores are designed to fulfil two key criteria: (i) their ability to select amongst ionic species; and (ii) ability to conduct ions at a high rate. Fortunately, biological ion channels which are abundant in nature, have been perfectly optimised by evolution to perform these tasks. Ion channels are holes through proteins, formed from thousands of atoms, and even minor mutations in structure can greatly influence their function and can be associated with disease [4]. Although it is clear that structure is a direct determinant of function, the mechanism through which this occurs has remained unclear and represents a major scientific challenge that we now address.

We will consider mixed sodium  $\text{Na}^+$  and calcium  $\text{Ca}^{++}$  transport and selectivity through the selectivity filter of a typical biological  $\text{Na}^+$  channel with 2 binding sites. In doing so, we will apply our multi-species equilibrium statistical theory [5]–[8], calculating the linear response conductivity from the fluctuations, using generalised Einstein relations. The development of theory in this area has already led to several important theoretical insights. These include the creation of a continuous statistical theory and its relationship with molecular dynamics [9], the analysis of selectivity through density functional theory [10], [11], and multi-species transport in narrow charged nanopores [12]–[15].

Leverhulme Trust Research Project Grant RPG-2017-134, Engineering and Physical Sciences Research Council Grant EP/M015831/1.

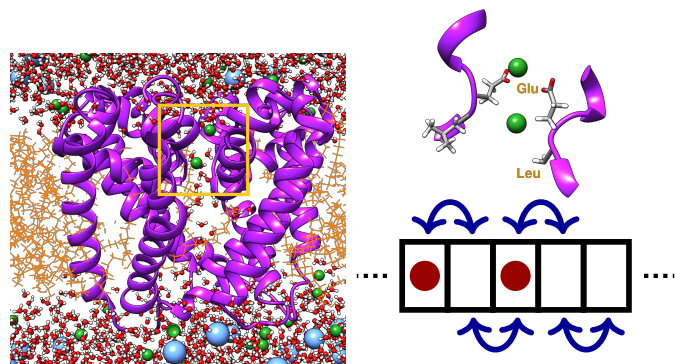


Fig. 1. Figure and caption taken from [7]. **Left**, structure of NaChBac [16], made using Chimera [17]. The protein (purple ribbons) is embedded into a lipid membrane (orange lines) and solvated on either side by a NaCl solution (blue and green spheres). **Right** and top, zoomed in view of the selectivity filter representing the pore (highlighted by the yellow box) and right bottom, the lattice approximation of the pore.

## II. THEORETICAL APPROACH

### A. Defining the system

We consider two bulk reservoirs with aqueous solutions containing ionic species  $i \in 1, \dots, S$ , diffusively and thermally coupled via a pore of volume  $V_c$  (see Fig. 1 taken from [7]). Under standard conditions the thermal de Broglie wavelength is smaller than system dimensions, and thus the system is classical and described by canonical statistics. The pore itself can be considered as a one-dimensional lattice with  $M$  binding sites, and individual site occupancy is characterised by the number  $n_{im}$ . We further assume that the steric properties of the site prohibit multiple ion occupancy and so  $n_{im} \in 0, 1$  for all  $m \in 1, \dots, M$  sites. As a result the total occupancy which is given by the double sum  $\sum_i \sum_m n_{im}$  represents a state of the system. If the sites are assumed to be identical then each state  $n_j$ , is defined by the total number of ions of each species in the pore and its total set is given by  $\{n_j\}$ .

Within the bulk the electrochemical potential can be calculated using Widom's insertion [18]. It contains contributions from the natural logarithm of the mole fraction  $x_i^b$ , the electric potential  $\phi^b$  and the excess chemical potential  $\bar{\mu}_i^b$ . This latter term provides the non-polar (surface tension and excluded volume) and electrostatic (Born and Debye-Hückel) contributions

to the solvation free energy [11], [19], [20]. Meanwhile we can establish two scales of interaction in the confined pore. It is known that pores repleted with charge (including total pore charge  $Q_f = n_f q$  where  $q$  is the proton charge) must reproduce strong electrostatic correlations  $\mathcal{E}$  [13], dependent on its geometry and total enclosed charge. However on the scale of the binding sites, the ions must also interact locally through short-range interactions  $\bar{\mu}_i^c$  including solvation and bonding [21].

### B. Energy spectrum

The total Gibbs free energy of each state can be expressed by writing the total energy and separating the degrees of freedom from the bulk and pore phases. Thus it reads as,

$$G(\{n_j\}; n_f) = \mathcal{E}(\{n_j\}; n_f) - \sum_i n_i \Delta \tilde{\mu}_i + \sum_i kT \ln(n_i)! + kT \ln\left(M - \sum_i n_i\right)!. \quad (1)$$

where:  $k$  and  $T$  are the Boltzmann constant and system temperature respectively and  $\Delta \tilde{\mu}_i$  is the summation of the difference in excess chemical potential between bulk and pore  $\Delta \tilde{\mu}_i = \bar{\mu}_i^b - \bar{\mu}_i^c$  plus the natural logarithm of the mole fraction. The final term represents the entropy of mixing for both the ions  $n_i$  and empty sites ( $n_w = M - \sum_i n_i$ ). We note that these energetic contributions are in exact agreement with the density functionals that are introduced to investigate ionic transport between charged surfaces and the related double layer effect see e.g. [22].

Here, we shall consider the form ( $\mathcal{E} = U_c(n_f + \sum_i z_i n_i)^2$ ), taken from [13], where  $U_c$  represents the capacitive charging energy, which is dependent on pore geometry and it takes the value of  $\sim 6kT$  in  $\text{Na}^+$  channels. It is of interest to note that this interaction is identical to that used in electron transport through quantum dots [23].

In (A) and (B) of Fig. 2 we display the free energy profiles for the full configuration of states. We consider  $\Delta \tilde{\mu}_{Ca} = 5kT$  and  $\Delta \tilde{\mu}_{Na} = 4kT$  and  $-20kT$  for (A) and (B) respectively. Solid blue and red lines represent pure  $\text{Ca}^{++}$  and  $\text{Na}^+$  states, whereas the mixed species states are presented in green. Each curve is parabolic in nature due to its quadratic dependence on  $n_f$ , and minimises when the total charge is neutralised i.e. equal to zero. Due to the difference in valence both  $\mathcal{E}$  and  $\Delta \tilde{\mu}_i$  govern the selectivity because these parameters translate the curves vertically and horizontally. To observe this let us consider the differences between (A) and (B). When  $\Delta \tilde{\mu}_{Na}$  is positive and comparable to  $\Delta \tilde{\mu}_{Ca}$ , the  $\text{Ca}^{++}$  levels are vertical translated when  $n_f$  is small due to the large electrostatic barrier; and hence unfavoured. Consequently the pure  $\text{Na}^+$  crossings occur at a lower energy (highlighted for the 0-1 transition by the purple circle at  $n_f \sim -0.1$ ). As this parameter is made strongly negative it imposes a blocking barrier for  $\text{Na}^+$  which ensures that the pure  $\text{Ca}^{++}$  crossings now occur at a lower energy and shifted value of  $n_f$ .

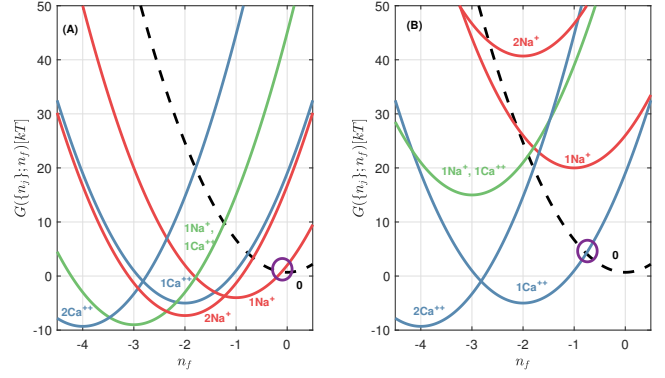


Fig. 2. Free energy vs.  $n_f$  for  $\Delta \tilde{\mu}_{Ca} \sim 5kT$  and with (A)  $\Delta \tilde{\mu}_{Na} \sim 4kT$  and (B)  $-20kT$ . The black dashed curve represents the ground state with 0 ions; and the blue, red and green curves represent  $\text{Ca}^{++}$ ,  $\text{Na}^+$ , and mixed states, respectively. Intersections of spectra correspond to degeneracies in energy, and the lowest energy intersection is highlighted by a purple circle.

### C. Statistical fluctuations and conductivity

The statistical fluctuations can be computed from the grand potential ( $\Omega = -kT \ln \mathcal{Z}$ ) which reads as follows,

$$\Omega = -kT \ln \left( \sum_{\{n_j\}} \left( \frac{1}{n_w!} \prod_i \frac{1}{n_i!} \right) e^{\frac{(\sum_i n_i \Delta \tilde{\mu}_i^b - \mathcal{E}(\{n_j\}; n_f))}{kT}} \right). \quad (2)$$

which includes the average number of ions in the pore of species  $i$  at constant system temperature and volume  $V$ ,

$$\langle n_i \rangle \equiv - \left( \frac{\partial \Omega}{\partial \eta_i^c} \right)_{T,V}. \quad (3)$$

together with the variance and covariance [20], [24],

$$\langle (\Delta n_i)^2 \rangle = \frac{\partial \langle n_i \rangle}{\partial \eta_i^c}, \quad \langle n_i n_j \rangle - \langle n_i \rangle \langle n_j \rangle = \frac{\partial \langle n_i \rangle}{\partial \eta_j^c}. \quad (4)$$

respectively. Here,  $\eta^c$  is the chemical potential in the pore which, at equilibrium, is equal to its bulk counterpart.

In multicomponent mixtures, non-equilibrium thermodynamics states that the Fickian diffusivity  $D_{ii}$  is related to the flux density  $j_i$  [15] via,

$$j_i = - \sum_{i=1}^S q \left( D_{ii} \nabla c_i + \sum_{j \neq i}^S D_{ij} \nabla c_j \right) - \sum_{i=1}^S \frac{\sigma_i}{z_i} \nabla \phi. \quad (5)$$

Here,  $c$  is the concentration in the pore ( $c_i = \langle n_i \rangle / V_c$ ). Cross diffusivities  $D_{ij}$  represent the ability for one species type to conduct in the presence of the concentration gradient for the other ion, and are equal to zero in independent solutions. We have shown in earlier work [5], [6], and it follows closely from [25], that the conductivity  $\sigma$  can be calculated under linear response conditions. If we assume that the kinetic properties of the ions are comparable such that  $D_{ii} \sim D_{jj} \sim D_{ij}$ , then the total conductivity through the pore at linear response

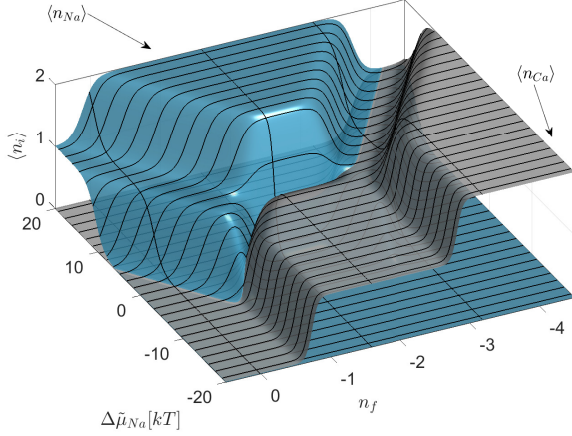


Fig. 3. Occupancy staircase for  $\text{Na}^+$  (blue) and  $\text{Ca}^{++}$  (grey) vs.  $n_f$  and  $\Delta\tilde{\mu}_{Na}$  with  $\Delta\tilde{\mu}_{Ca} = 5kT$ . Plateaus correspond to stability with the pore being locked into one state, meanwhile steps correspond to energies at which the pore can reside in multiple states.

$\sigma = \sum_{i=1}^S \sigma_i$ , is proportional to the variance in total particle number i.e.

$$\sigma \propto \left( \sum_i^S \frac{\partial \langle n_i \rangle}{\partial \eta_i^c} + \sum_{j \neq i}^S \frac{\partial \langle n_j \rangle}{\partial \eta_i^c} \right). \quad (6)$$

### III. ANALYSIS

To investigate the selective properties of the pore we should also analyse both the mean number of ions (occupancy) of  $\text{Na}^+$  (blue) and  $\text{Ca}^{++}$  (grey) in Fig. 3, and the variance of total particle number in Fig. 4 (which is proportional to the conductivity Eqn. (6)), vs.  $\Delta\tilde{\mu}_{Na}$  and  $n_f$ , with  $\Delta\tilde{\mu}_{Ca} = 5kT$ .

Occupancy forms a staircase, where plateaus correspond to integer values of ions in the pore. As  $n_f$  becomes more negative the total number of ions residing in the pore increases because of the increased electrostatic attraction to the pore. As we have already seen the selectivity is defined by both  $\mathcal{E}$  and  $\Delta\tilde{\mu}$ . To observe this let us consider  $n_f = -2$  because the electrostatic interaction can then be neutralised with either 1  $\text{Ca}^{++}$  ion or 2  $\text{Na}^+$  ions. Consequently when  $\Delta\tilde{\mu}_{Na} \lesssim \Delta\tilde{\mu}_{Ca}/2$  the pore favours  $\text{Ca}^{++}$ . Non-selectivity occurs when each of the species states are energetically indistinguishable and so the vertical steps for each species converge. An example of this occurs when  $\Delta\tilde{\mu}_{Na} \sim -4kT$  and  $n_f \sim 0.8$ .

As shown in Fig. 4, the variance in particle number forms a complicated structure with two sets of peaks ( $T_1$  and  $T_2$ ) corresponding to 0-1 and 1-2 ion transitions, that are separated by a region of negligible conductivity. Peaks form at the midpoints of the vertical occupancy steps where there is a change in total number of ions in the pore, i.e. a step in the total occupancy. This result is intuitively clear, because these points correspond to degeneracies in the system, when adding or removing an ion does not cost any energy. Away from these points there is a corresponding energy barrier impeding conduction. As a result we can establish two conditions on that

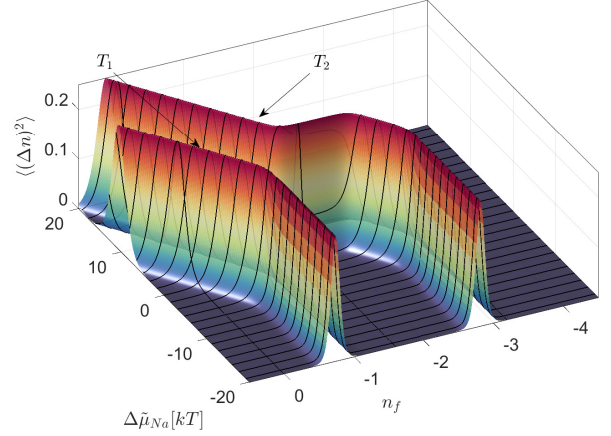


Fig. 4. Variance in total particle number vs.  $n_f$  and  $\Delta\tilde{\mu}_{Na}$  with  $\Delta\tilde{\mu}_{Ca} = 5kT$ . Peaks corresponding to transitions between 0-1 and 1-2 ions in the pore are labelled  $T_1$  and  $T_2$ .

must be satisfied for optimal conductivity: (i) the pore must be degenerate i.e.  $\Delta G \sim 0$  and (ii) both states must correspond to the favoured occupancy's of the pore i.e. lowest free energy (see purple circles in Fig. 2). Since this occurs between neighbouring states it also corresponds directly to knock-on conduction. Collectively these phenomena are known as *ionic Coulomb blockade* a classical analogy [26]–[28] of the process observed in electron transport [23].

The structure of the peaks differs because  $T_2$  allows for conduction involving mixed states. As a result, it can produce  $\text{Na}^+$  conduction between the pure (1 $\text{Na}^+$  and 2 $\text{Na}^+$ ) and mixed (1 $\text{Ca}^{++}$  and 1 $\text{Ca}^{++}$ 1 $\text{Na}^+$ ) states and pure  $\text{Ca}^{++}$  conduction. Mixed state conduction between these states has been qualitatively observed in simulations of  $\text{Na}^+$  channels. In [29], the system was initiated with both  $\text{Na}^+$  and  $\text{Ca}^{++}$  present in the pore, and  $\text{Na}^+$  was shown to bypass the resident  $\text{Ca}^{++}$  ion, in a similar manner to [30]. Finally we must note that the branch parallel to  $n_f$  appears to suggest an anomalous conduction event. This branch occurs when  $-1.4 \lesssim n_f \lesssim -2.1$  and  $\Delta\tilde{\mu}_{Na} \sim -2.8kT$ , and corresponds to the degeneracy between the 1 $\text{Ca}^{++}$  and 2 $\text{Na}^+$  states. As a result conduction does not occur via the knock-on mechanism. It's importance and implications will be further explored in future work.

These properties can be combined to generate a phase diagram, further helping to elucidate the picture, Fig. 5. The coloured blocks correspond to the occupancy and are labelled, meanwhile the purple regions denote instability because the pore can reside in multiple states of different numbers of particles. As a result there is a quasi-phase-boundary separating different locations of non-zero conductivity. The blue and orange lines correspond to the midpoint of the  $\text{Na}^+$  and  $\text{Ca}^{++}$  occupancy step, and the black line corresponds to the maximal conductivity. It is clear that the pore switches from  $\text{Na}^+$  to  $\text{Ca}^{++}$  conduction when  $\Delta\tilde{\mu}_{Na} \lesssim -6kT$ , and that mixed state conduction occurs when the mixed state is the

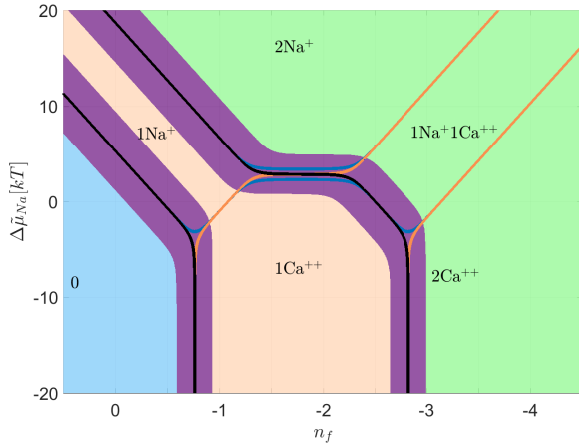


Fig. 5. Phase diagram of the pore. Coloured blocks refer to its occupancy, with purple denoting locations where it is made from a superposition of  $n$  and  $n + 1$  ions. Blue and orange lines correspond to the midpoint of the  $\text{Na}^+$  and  $\text{Ca}^{++}$  occupancy steps, and the black lines displays the maximal conductivity.

favoured 2 ion state which occurs when  $-2.1 \lesssim n_f \lesssim -2.7$ .

#### IV. CONCLUSION

In conclusion, we have investigated the mixed-valence transport properties of narrow ion channels, through analysis of a multi-component statistical and linear response theory. In particular we have focused on  $\text{Na}^+$  vs.  $\text{Ca}^{++}$  selectivity in a typical biological  $\text{Na}^+$  channel. Strong selectivity is observed in both the variance in total particle number and the mean number of ions in the pore. This is determined by both the electrostatic interaction because the ions have a differing valence, and also the local interactions. We can identify two conditions required for optimal selective transport: (i) the pore must be degenerate i.e.  $\Delta G \sim 0$  and (ii) both states must correspond to the energetically favoured occupancy of the pore i.e. lowest free energy. Therefore, it is possible to predict the pore changes required to shift the selectivity and/or the conduction mechanism.

In future we will further analyse the far-from-equilibrium regime through the development of a master equation model. Finally we expect that the proposed formalism should also be applicable to other artificial nano-pores or biological channels.

#### REFERENCES

- [1] D. Deamer, M. Akeson, and D. Branton, "Three decades of nanopore sequencing," *Nat. Biotechnol.*, vol. 34, no. 5, pp. 518–524, 2016.
- [2] M. S. Mauter, I. Zucker, F. Perreault, J. R. Werber, J.-H. Kim, and M. Elimelech, "The role of nanotechnology in tackling global water challenges," *Nat. Sustain.*, vol. 1, no. 4, pp. 166–175, 2018.
- [3] R. W. Baker, "Future directions of membrane gas separation technology," *Ind. Eng. Chem. Res.*, vol. 41, no. 6, pp. 1393–1411, 2002.
- [4] F. M. Ashcroft, *Ion Channels and Disease*. Academic press, 1999.
- [5] D. G. Luchinsky, W. A. T. Gibby, I. Kaufman, D. A. Timucin, and P. V. E. McClintock, "Statistical theory of selectivity and conductivity in biological channels," *arXiv preprint arXiv:1604.05758*, 2016.
- [6] D. G. Luchinsky, W. A. T. Gibby, I. K. Kaufman, P. V. E. McClintock, and D. A. Timucin, "Relation between selectivity and conductivity in narrow ion channels," in *2017 International Conference on Noise and Fluctuations (ICNF)*, 2017, pp. 1–4.

- [7] W. A. T. Gibby, M. Barabash, C. Guardiani, D. Luchinsky, O. Fedorenko, S. K. Roberts, and P. V. E. McClintock, "Theory and experiments on multi-ion permeation and selectivity in the NaChBac ion channel," *Fluctuation Noise Lett.*, vol. 18, no. 2, p. 1940007, 2019.
- [8] W. A. T. Gibby, M. L. Barabash, C. Guardiani, D. G. Luchinsky, and P. V. E. McClintock, "The role of noise in determining selective ionic conduction through nano-pores," in *2018 IEEE 13th Nanotechnology Materials and Devices Conference (NMDC)*, Oct 2018, pp. 1–6.
- [9] B. Roux, "Statistical mechanical equilibrium theory of selective ion channels," *Biophys. J.*, vol. 77, no. 1, pp. 139–153, 1999.
- [10] D. Gillespie and R. Eisenberg, "Physical descriptions of experimental selectivity measurements in ion channels," *Euro. Biophys. J.*, vol. 31, no. 6, pp. 454–466, 2002.
- [11] D. Gillespie, "Energetics of divalent selectivity in a calcium channel: The ryanodine receptor case study," *Biophys. J.*, vol. 94, no. 4, pp. 1169–1184, 2008.
- [12] J. Zhang, A. Kamenev, and B. I. Shklovskii, "Conductance of Ion Channels and Nanopores with Charged Walls: A Toy Model," *Phys. Rev. Lett.*, vol. 95, p. 148101, 2005.
- [13] —, "Ion exchange phase transitions in water-filled channels with charged walls," *Phys. Rev. E*, vol. 73, p. 051205, 2006.
- [14] T. Becker, K. Nelissen, B. Cleuren, B. Partoens, and C. Van den Broeck, "Diffusion of interacting particles in discrete geometries," *Phys. Rev. Lett.*, vol. 111, p. 110601, Sep 2013.
- [15] S. R. De Groot and P. Mazur, *Non-equilibrium thermodynamics*. Courier Corporation, 2013.
- [16] C. Guardiani, P. M. Rodger, O. A. Fedorenko, S. K. Roberts, and I. A. Khovanov, "Sodium binding sites and permeation mechanism in the NaChBac channel: A molecular dynamics study," *J. Chem. Theor. Comp.*, pp. 1389–1400, 2016.
- [17] E. F. Pettersen, T. D. Goddard, C. C. Huang, G. S. Couch, D. M. Greenblatt, E. C. Meng, and T. E. Ferrin, "UCSF Chimera - a visualization system for exploratory research and analysis," *J. Comput. Chem.*, vol. 25, no. 13, pp. 1605–1612, 2004.
- [18] B. Widom, "Potential-distribution theory and the statistical mechanics of fluids," *J. Phys. Chem.*, vol. 86, no. 6, pp. 869–872, 1982.
- [19] B. Roux, T. Allen, S. Berneche, and W. Im, "Theoretical and computational models of biological ion channels," *Quart. Rev. Biophys.*, vol. 37, no. 1, pp. 15–103, 2004.
- [20] D. A. McQuarrie, *Statistical Mechanics*. Sausalito CA: University Science Books, 2000.
- [21] P. D. Dixit, S. Merchant, and D. Asthagiri, "Ion selectivity in the KcsA potassium channel from the perspective of the ion binding site," *Biophys. J.*, vol. 96, no. 6, pp. 2138–2145, 2009.
- [22] J.-S. Sin, Y.-M. Jang, C.-H. Kim, and H.-C. Kim, "Steric effect of water molecule clusters on electrostatic interaction and electroosmotic transport in aqueous electrolytes: A mean-field approach," *AIP Advances*, vol. 8, no. 10, p. 105222, 2018.
- [23] C. W. J. Beenakker, "Theory of Coulomb-blockade oscillations in the conductance of a quantum dot," *Phys. Rev. B*, vol. 44, no. 4, pp. 1646–1656, 1991.
- [24] L. D. Landau and E. M. Lifshitz, *Statistical Physics. Course of Theoretical Physics*. Volume 5. Third edition, Part I. Oxford: Pergamon Press, 1980.
- [25] P. T. Landsberg, "Einstein and statistical thermodynamics. III. The diffusion-mobility relation in semiconductors," *Eur. J. Phys.*, vol. 2, no. 4, p. 213, 1981.
- [26] I. K. Kaufman, P. V. E. McClintock, and R. S. Eisenberg, "Coulomb blockade model of permeation and selectivity in biological ion channels," *New J. Phys.*, vol. 17, no. 8, p. 083021, 2015.
- [27] I. K. Kaufman, O. A. Fedorenko, D. G. Luchinsky, W. A. T. Gibby, S. K. Roberts, P. V. E. McClintock, and R. S. Eisenberg, "Ionic Coulomb blockade and anomalous mole fraction effect in the NaChBac bacterial ion channel and its charge-varied mutants," *EPJ Nonlinear Biomedical Physics*, vol. 5, p. 4, 2017.
- [28] N. Kavokine, S. Marbach, A. Siria, and L. Bocquet, "Ionic Coulomb blockade as a fractional Wien effect," *Nat. Nanotechnol.*, p. 1, 2019.
- [29] C. Guardiani, O. A. Fedorenko, S. K. Roberts, and I. A. Khovanov, "On the selectivity of the NaChBac channel: an integrated computational and experimental analysis of sodium and calcium permeation," *Phys. Chem. Chem. Phys.*, vol. 19, no. 44, pp. 29 840–29 854, 2017.
- [30] B. Corry, " $\text{Na}^+/\text{Ca}^{2+}$  selectivity in the bacterial voltage-gated sodium channel NavAb," *PeerJ*, vol. 1, p. e16, 2013.